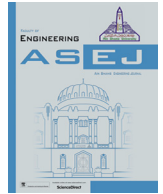




Contents lists available at ScienceDirect

Ain Shams Engineering Journal

journal homepage: www.sciencedirect.com



Engineering Physics and Mathematics

Three-dimensional flow of Jeffrey fluid between a rotating and stationary disks with suction

P. Maninaga Kumar, A. Kavitha*

Department of Mathematics, School of Advanced Sciences, VIT University, Vellore, Tamil Nadu 632014, India

ARTICLE INFO

Article history:

Received 11 August 2016

Revised 6 March 2017

Accepted 2 April 2017

Available online xxxxx

Keywords:

Jeffrey fluid
Skin-friction
Circular disks
Creeping flow

ABSTRACT

A three-dimensional steady flow of an incompressible Jeffrey fluid bounded by two parallel circular disks, one rotating and other stationary is examined with uniform suction at the stationary disk. Solutions for the governing equations are obtained applying "Power series method". The velocity distributions, pressure coefficient and skin frictions are obtained which in turn are compared with assumptions of creeping flow solutions. The velocity distribution and pressure coefficient are discussed graphically. We found that the radial velocity increases and axial velocity decreases when Jeffrey parameter is increased.

© 2017 Production and hosting by Elsevier B.V. on behalf of Ain Shams University. This is an open access article under the CC BY-NC-ND license (<http://creativecommons.org/licenses/by-nc-nd/4.0/>).

1. Introduction

The flow of an incompressible fluid bounded by parallel disks whether porous or non-porous has been extensively investigated so far by many researchers. The classical study of Stewartson [1] presented fixed motion of viscous fluid restrained by two coaxial rotating disks is discussed both experimentally and theoretically. Pearson [2] has repeatedly discussed the character of the steady-state viscous flow bounded by two large rotating disks by using a type of the numerical method expressed in digital computer solutions for the time-dependent case. Elkouh [3] has elucidated the equation of motion for a firm, incompressible, axially symmetric flow of a fluid bounded by parallel porous disks. The flow is entirely the result of either suction or injection throughout the disks. Mellor et al. [4] experimented the flow between two coaxial infinite disks, in which one is rotating and other is stationary. Rudraiah [5] has discussed three-dimensional flows between a rotating and a stationary disk with uniform suction at the stationary disk. He got solutions for the Navier-Stokes equations and the expressions for the velocity, pressure coefficients and skin-friction

are compared with the solutions based on the assumptions of creeping flow.

Mishra et al. [6] studied about a laminar flow of incompressible elastico-viscous fluid which is flown between a porous rotating disk and non-porous stationary disk. Herethe effects of rotation coefficient, velocity components, radial pressure variation and shear stress at the disks are observed. Hayat et al. [7] conducted an experiment in which the effects of an endoscope and magnetic field on the peristalsis involving Jeffrey fluid. Here he described the accurate analytic result for velocity components and pressure gradient. Nadeem et al. [8] found that the incompressible Jeffrey fluids and the effects of variable viscosity are supposed to vary as an exponential function of temperature. The governing fundamental equations are estimated under the long wavelength and low Reynolds number.

Vajravelu et al. [9] studied the peristaltic flow of Jeffrey fluid in a vertical porous stratum with heat transfer under long wavelength and low Reynolds number. The effects of various parameters on the velocity, temperature and the pumping characteristics are discussed. Farooq et al. [10] researched about the influence of couple stresses on the flow of fluid in which an infinite disk is rotating at a constant angular velocity. Kavitha et al. [11] discussed the peristaltic pumping of a non-Newtonian Jeffrey fluid between two permeable walls with suction and injection. The effect of suction/ injection parameter, amplitude ratio and permeability parameter including slip on flow quantities are evaluated. Qayyum et al. [12] studied the vacillating axisymmetric flow of Jeffrey fluid between two parallel disks.

* Corresponding author.

E-mail address: kavitha@vit.ac.in (A. Kavitha).

Peer review under responsibility of Ain Shams University.



Production and hosting by Elsevier

<http://dx.doi.org/10.1016/j.asej.2017.04.003>

2090-4479/© 2017 Production and hosting by Elsevier B.V. on behalf of Ain Shams University.

This is an open access article under the CC BY-NC-ND license (<http://creativecommons.org/licenses/by-nc-nd/4.0/>).

Please cite this article in press as: Maninaga Kumar P, Kavitha A. Three-dimensional flow of Jeffrey fluid between a rotating and stationary disks with suction. Ain Shams Eng J (2017), <http://dx.doi.org/10.1016/j.asej.2017.04.003>

Ellahi et al. [13] investigated Mathematical Modelling of Magneto-Hydrodynamic peristaltic flow of Jeffrey fluid in the space between two eccentric tubes in the presence of magnetic field. Siddiqui et al. [14] studied classical Von Kármán flow of Jeffrey fluid by using a generalized non-similarity transformation. He concluded that the boundary layer structure develops near the surface of the disk and far-field behavior is distinct from the near-wall solution. Ellahi et al. [15] examined numerical models of Jeffrey liquid by means of nanoparticles in the stenosed atherosclerotic conduits. The convection impacts of warmth exchange with the catheter are additionally considered. Riaz et al. [16] deduced precise answers for the peristaltic stream of Jeffrey liquid model in a cross-sectional area of a three dimensional rectangular channel having a slip at the peristaltic limits. Nadeem et al. [17] studied Jeffrey liquid model with nanoparticles in peristaltic waves of a three-dimensional rectangular channel.

Rashidi et al. [18] evaluated a scientific model for two-dimensional liquid stream affected by stream astute transverse attractive fields in a laminar flow. Nawaz et al. [19] studied the Joules warming consequences for stagnation point stream of Newtonian and non-Newtonian liquids over an extending chamber by the method for genetic algorithm (GA). Ellahi et al. [20] studied the magnetohydrodynamics Couette flow of Eyring – Powell fluid with heat transfer Couette stream. Here the outcomes for the zero liquid slip and no warm slip are determined. Bhatti et al. [21] presented the impacts of a variable magnetic field on the peristaltic stream of Jeffrey liquid in a non-uniform rectangular conduit having consistent dividers. Rahman et al. [22] analyzed the impacts of nanoparticles for the blood stream of Jeffrey liquid in decreased course with **stenosis**. The slip impacts alongside penetrable nature of the blood vessel divider within the sight of convection are likewise considered.

In the existing paper, the three-dimensional flow of an incompressible Jeffrey fluid bounded by two circular disks, one rotating and the other stationary is examined with a uniform suction at the stationary disk. The motion is three-dimensional due to the rotation of a disk. The fluid is thrown outward by centrifugal force. The fluid moves towards the disk in the axial direction to replace the fluid that is thrown out. The solution for creeping flow are obtained and are compared with those of non-creeping flow solutions. Furthermore, it is apparent that many other solutions for a rotation Reynolds number are possible.

2. Mathematical formulation

The governing Eqs. (Rudraiah 1969 [5]) which are based on axial symmetry are

$$\frac{1}{r} \frac{\partial}{\partial r}(rU_r) + \frac{\partial U_z}{\partial z} = 0. \tag{1}$$

$$U_r \frac{\partial U_r}{\partial r} + U_z \frac{\partial U_r}{\partial z} - \frac{U_\theta^2}{r} = -\frac{1}{\rho} \frac{\partial p}{\partial r} + \frac{\nu}{1 + \lambda_1} \left[\frac{\partial^2 U_r}{\partial r^2} + \frac{\partial}{\partial r} \left(\frac{U_r}{r} \right) + \frac{\partial^2 U_r}{\partial z^2} \right]. \tag{2}$$

$$\frac{U_r}{r} \frac{\partial(rU_\theta)}{\partial r} + U_z \frac{\partial U_\theta}{\partial z} = \frac{\nu}{1 + \lambda_1} \left[\frac{\partial^2 U_\theta}{\partial r^2} + \frac{\partial}{\partial r} \left(\frac{U_\theta}{r} \right) + \frac{\partial^2 U_\theta}{\partial z^2} \right]. \tag{3}$$

$$U_r \frac{\partial U_z}{\partial r} + U_z \frac{\partial U_z}{\partial z} = -\frac{1}{\rho} \frac{\partial p}{\partial z} + \frac{\nu}{1 + \lambda_1} \left[\frac{\partial^2 U_z}{\partial r^2} + \frac{1}{r} \frac{\partial U_z}{\partial r} + \frac{\partial^2 U_z}{\partial z^2} \right]. \tag{4}$$

The disk $z = 1$ is rotating while the disk $z = 0$ is stationary. The fluid is extracted with a uniform velocity U through the latter disk.

If Ω is the angular velocity of the disk $z = 1$, the boundary conditions are

$$U_r(r, 0) = 0, \quad U_r(r, 1) = 0. \tag{5}$$

$$U_\theta(r, 0) = 0, \quad U_\theta(r, 1) = \Omega r. \tag{6}$$

$$U_z(r, 0) = -U, \quad U_z(r, 1) = 0. \tag{7}$$

Using the transformations:

$$\begin{aligned} z &= l\xi, \\ U_\theta &= \Omega r g(\xi), \\ U_z &= -U f(\xi), \\ U_r &= \frac{Ur}{2l} f'(\xi), \end{aligned} \tag{8}$$

Eqs. (2) to (4) become

$$\frac{1}{(1 + \lambda_1)R} f''' + ff'' - \frac{1}{2} f'^2 = \frac{2l^2}{\rho U^2 r} \frac{\partial p}{\partial r} - \frac{2R_1^2}{R^2} g^2. \tag{9}$$

$$\frac{1}{(1 + \lambda_1)R} g'' - f'g + fg' = 0. \tag{10}$$

$$\frac{1}{(1 + \lambda_1)R} f'' + ff' = -\frac{1}{\rho U^2} \frac{\partial p}{\partial z}. \tag{11}$$

where $R = \frac{Ul}{\nu}$ is the suction Reynolds number and $R_1 = \frac{\Omega l^2}{\nu}$ is the rotation Reynolds number.

Since the left side of Eq. (11) is a function of z only, so that Eq. (9) becomes

$$f''' + R(1 + \lambda_1) \left(ff'' - \frac{1}{2} f'^2 \right) = C - \lambda(1 + \lambda_1) R g^2. \tag{12}$$

where C is the constant of integration and $\lambda = \frac{2R_1^2}{R^2}$. \tag{13}

The corresponding boundary conditions will be

$$\begin{aligned} f'(0) &= 0, \quad f'(1) = 0, \\ g(0) &= 0, \quad g(1) = 1, \\ f(0) &= 1, \quad f(1) = 0. \end{aligned} \tag{14}$$

Solution for R:

The solution for Eqs. (10) and (12) can be expressed for small values of R with a finite λ by a power series developed near $R = 0$ as follows

$$f = \sum_{n=0}^{\infty} R^n f_n, \quad g = \sum_{n=0}^{\infty} R^n g_n, \quad C = \sum_{n=0}^{\infty} R^n C_n, \tag{15}$$

Eqs. (12) and (10) using (15) become

$$\sum_{n=0}^{\infty} R^n f_n''' + \sum_{n=0}^{\infty} R^n (1 + \lambda_1) \sum_{r=0}^{n-1} \left[f_r f_{n-r-1}'' - \frac{1}{2} f_r' f_{n-r-1}' + \lambda g_r g_{n-r-1} \right] = \sum_{n=0}^{\infty} R^n C_n. \tag{16}$$

$$\sum_{n=0}^{\infty} R^n g_n'' + \sum_{n=0}^{\infty} R^n (1 + \lambda_1) \sum_{r=0}^{n-1} [f_r g_{n-r-1}' - f_r' g_{n-r-1}] = 0. \tag{17}$$

The boundary conditions satisfied by f_n 's and g_n 's are:

$$\begin{aligned} f_n'(0) &= 0, \quad f_n'(1) = 0, \\ g_n(0) &= 0, \quad g_n(1) = 1, \quad g_n(1) = 0, \quad \text{for } n > 0 \\ f_0(0) &= 1, \quad f_0(1) = 0 \quad \text{for } n > 0, \quad f_n(1) = 0. \end{aligned} \tag{18}$$

The solutions of (16) and (17) are

$$f(\xi) = (2\xi^3 - 3\xi^2 + 1) + \frac{R(1+\lambda_1)}{420}[-12\xi^7 + 42\xi^6 - 7\lambda\xi^5 - 210\xi^4 + (21\lambda + 312)\xi^3 - (132 + 14\lambda)\xi^2] + R^2(1 + \lambda_1)^2 \times \left[\frac{3}{1925}\xi^{11} - \frac{3}{350}\xi^{10} + (6 - \frac{\lambda}{30})\frac{\xi^9}{504} + (\frac{36}{5} - \frac{\lambda}{10})\frac{\xi^8}{336} - (\frac{192}{35} + \frac{\lambda}{10})\frac{\xi^7}{70} + (\frac{40}{7} + \frac{53\lambda}{30})\frac{\xi^6}{120} \right] + \dots$$

And

$$g(\xi) = \xi + \frac{R(1+\lambda_1)}{20}[4\xi^5 - 5\xi^4 - 10\xi^2 + 11\xi] + \frac{R^2(1+\lambda_1)^2}{25200} \left[\begin{matrix} -340\xi^9 + 1260\xi^8 - (40\lambda + 900)\xi^7 - 2940\xi^6 \\ + (5760 + 126\lambda)\xi^5 - (70\lambda + \frac{55}{336})\xi^4 + 4200\xi^3 \\ - 6930\xi^2 + (2935 - 16\lambda)\xi \end{matrix} \right] + \dots$$

With

$$C = 12 + \left(\frac{3\lambda}{10} - \frac{54}{35}\right)R(1 + \lambda_1) + \left(-\frac{69}{1078} + \frac{683\lambda}{1575}\right)R^2(1 + \lambda_1)^2 + \dots \quad (21)$$

where a second order perturbation solution is considered sufficiently accurate.

The solutions for the creeping flow are

$$f(\xi) = (2\xi^3 - 3\xi^2 + 1). \quad (22)$$

$$g(\xi) = \xi. \quad (23)$$

$$C = 12. \quad (24)$$

The torque on the rotating disk can be evaluated from the shearing stress component $\tau_{z\theta}$ which acts in the place of the disk and produces a force in θ direction.

$$\tau_{z\theta} = \rho \frac{v}{(1 + \lambda_1)} \left[\frac{1}{r} \frac{\partial U_z}{\partial \theta} + \frac{\partial U_\theta}{\partial z} \right]_{z=l} = \rho \frac{v}{(1 + \lambda_1)} \left[\frac{\partial U_\theta}{\partial z} \right]_{z=l} = \frac{\rho v \Omega r}{l(1 + \lambda_1)} g'(1). \quad (25)$$

If the edge effects are neglected the torque on the disk of radius r_0 wetted on both sides is:

$$T = 2 \int_0^{r_0} (\tau_{z\theta})_l 2\pi r^2 dr = \frac{\Pi \rho \Omega g'(1)}{l(1 + \lambda_1)} r_0^4. \quad (26)$$

The pressure coefficient C_p is

$$C_p = \frac{P(r, \lambda) - P(r, 1)}{\mu U/l} \frac{l^2}{\alpha^2} = \left[3 + \left(\frac{3\lambda}{40} - \frac{27}{70}\right)R(1 + \lambda_1) \right] \left(1 - \frac{r^2}{\alpha^2} \right). \quad (27)$$

where

$$P(r, \lambda) - P(r, 1) = \frac{\mu U}{4l^3} \left[12 + \left(\frac{3\lambda}{10} - \frac{54}{35}\right)R(1 + \lambda_1) \right] (r^2 - \alpha^2). \quad (28)$$

The pressure coefficient for the creeping flow is:

$$C_p = 3 \left(1 - \frac{r^2}{\alpha^2} \right). \quad (29)$$

The components of skin-friction in the radial and azimuthal directions at the plane $z = 0$ are:

$$C_\tau^0 = \left[\frac{6}{35} - \frac{6}{R(1 + \lambda_1)} - \frac{\lambda}{15} \right] \frac{r}{\alpha}. \quad (30)$$

$$C_\theta^0 = \frac{1}{R_1} \left(2 + \frac{11R(1 + \lambda_1)}{10} \right) \frac{r}{\alpha}. \quad (31)$$

And the plate $z = 1$ are:

$$C_\tau^1 = \left[\frac{6}{R(1 + \lambda_1)} - \left(\frac{81}{105} + \frac{\lambda}{10} \right) \right] \frac{r}{\alpha}. \quad (32)$$

$$C_\theta^1 = \frac{1}{R_1} \left(2 - \frac{9R(1 + \lambda_1)}{10} \right) \frac{r}{\alpha}. \quad (33)$$

These expressions for creeping flow are:

$$C_\tau^0 = \left[-\frac{6}{R(1 + \lambda_1)} \right] \frac{r}{\alpha}. \quad (34)$$

$$C_\theta^0 = 0. \quad (35)$$

$$C_\tau^1 = \frac{6}{R(1 + \lambda_1)} \frac{r}{\alpha}. \quad (36)$$

$$C_\theta^1 = \frac{2}{R_1} \frac{r}{\alpha}. \quad (37)$$

For a creeping flow the torque τ_0 is:

$$T_0 = \frac{\pi \rho v \Omega r_0^4}{(1 + \lambda_1) l}. \quad (38)$$

3. Results & discussion

In this paper, the study of three dimensional flow of Jeffrey fluid bounded by two parallel disks one rotating and other stationary with suction is investigated. The governing Eqs. are transformed by using the transformation Eq. (8), resulting Eqs. are (9)–(11). By using “Power series method”, we get $f(\xi)$, $g(\xi)$ and are given Eqs. (19) and (20). From the above Eqs. velocity distribution is obtained. In the Eq. (28), the pressure distribution is found and the components of skin frictions are presented in Eqs. (30)–(33)

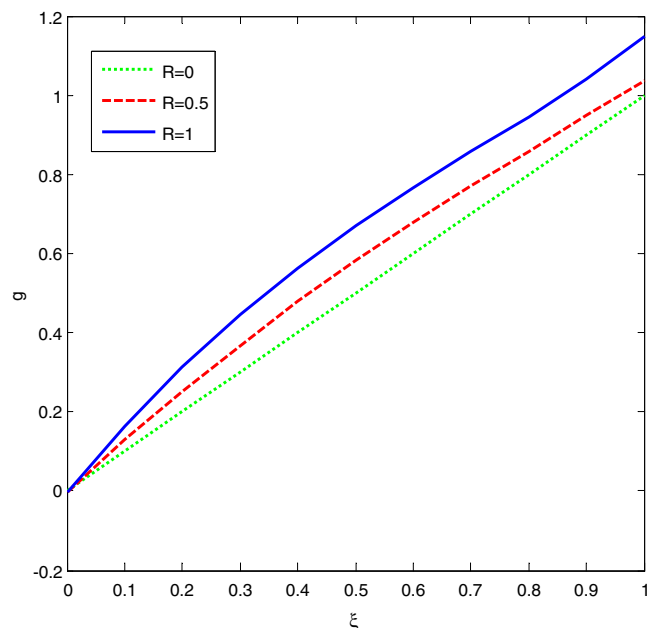


Figure 1. The variation of azimuthal velocity with ξ for different values of Reynolds number with $\lambda = 1, \lambda_1 = 0.1$.

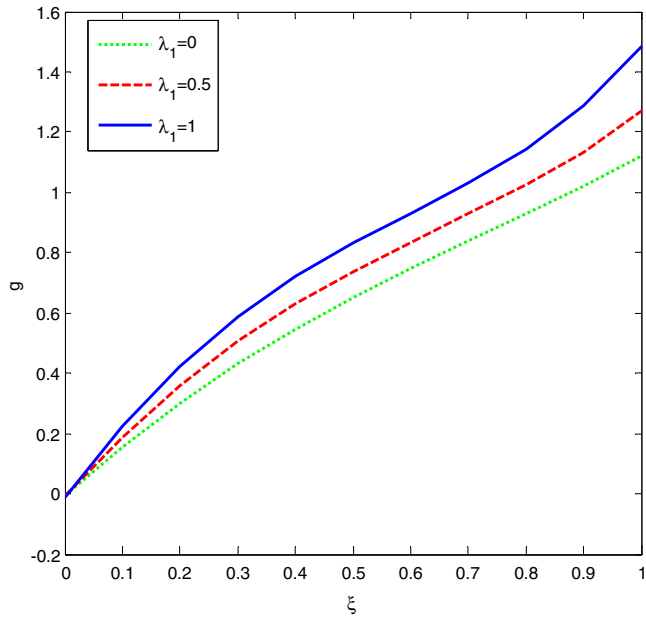


Figure 2. The variation of azimuthal velocity with ξ for different values of Jeffrey parameter λ_1 with $\lambda = 1, R = 1$.

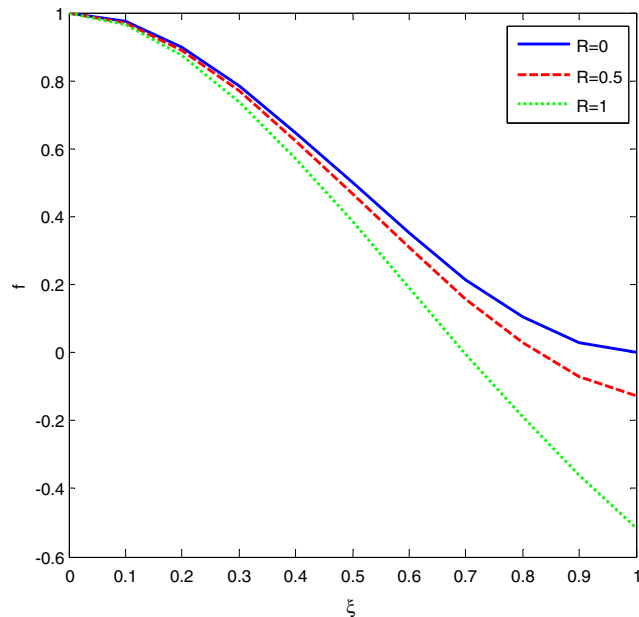


Figure 3. The variation of axial velocity with ξ for different values of Reynolds Number with $\lambda = 1, \lambda_1 = 0.1$.

and compared with the assumptions of creeping flow. The results are shown graphically from Figs. 1–6 for the Velocity distribution and Figs. 7 and 8 for the pressure distributions.

Fig. 1 is plotted to see the influence of suction Reynolds number on the azimuthal velocity for fixed values $\lambda = 1$ and $\lambda_1 = 0.1$. It is observed that the azimuthal velocity is increasing with the increase of suction Reynolds number.

Fig. 2 is sketched to find the effect of Jeffrey parameter λ_1 on the azimuthal velocity for fixed parameter $\lambda = 1$ and $R = 1$. It is observed that the azimuthal velocity is increasing with the increase of Jeffrey parameter.

Fig. 3 is illustrated to find the effect of influence of suction Reynolds number on axial velocity for fixed values $\lambda = 1$ and $\lambda_1 = 0.1$.

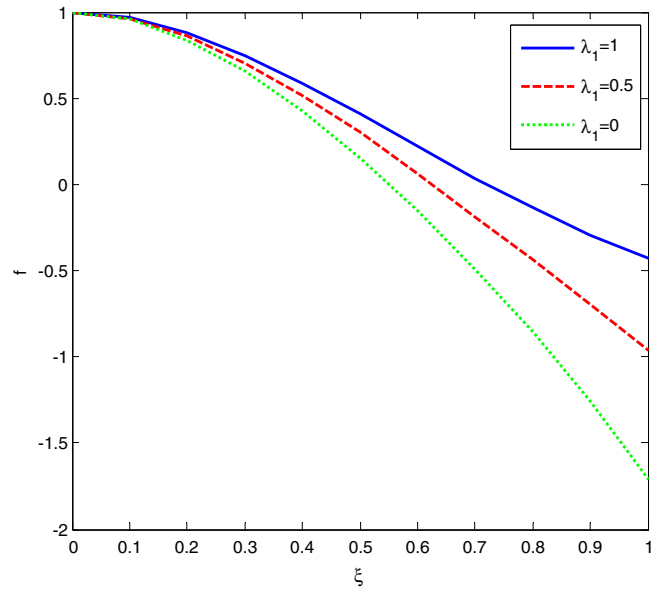


Figure 4. The variation of axial velocity with ξ for different values of Jeffrey Parameter λ_1 with $\lambda = 1, R = 1$.

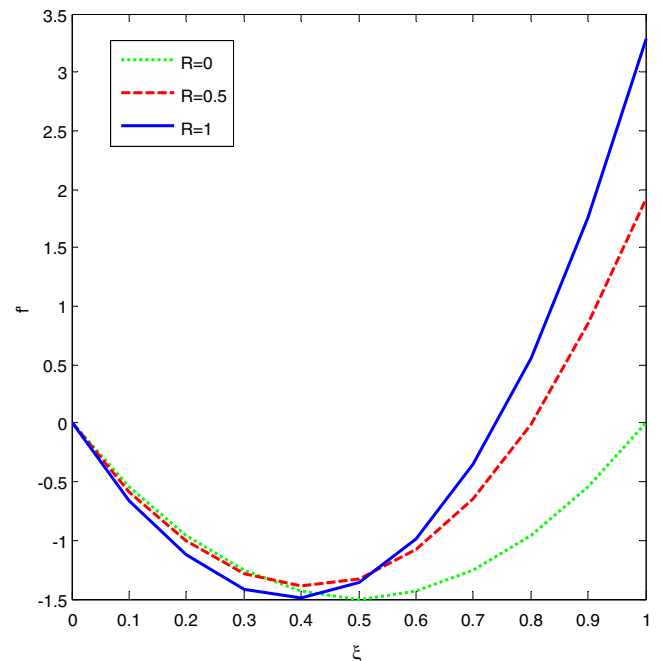


Figure 5. The variation of radial velocity with ξ for different values of Reynolds Number with $\lambda = 1, \lambda_1 = 0.1$.

It is shown that the axial velocity is decreasing with the increase of suction Reynolds number. It is due to the fact that as we increase the suction Reynolds number, the inertial force increases which reduce the fluid motion, further upper disk is rotating and lower disk is stationary so that axial velocity decreasing.

Fig. 4 is plotted to see the effect of Jeffrey parameter λ_1 the effect is to enhance the axial velocity of the flow between rotating and stationary disks for given values $\lambda = 1$ and $R = 1$.

The behavior of radial velocity for suction Reynolds number R is described in Fig. 5. Magnitude of radial velocities decays at stationary disk with an increase R . This may due to effect of inertial forces acting in the fluid with fixed values of $\lambda = 1$ and $\lambda_1 = 0.1$.

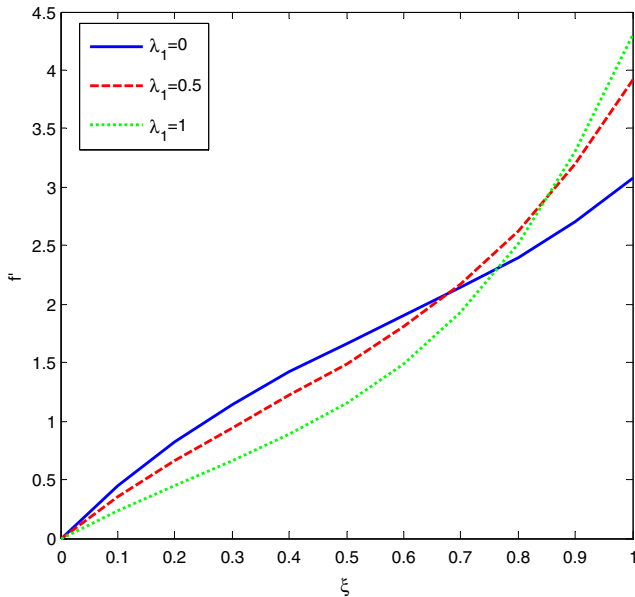


Figure 6. The variation of radial velocity with ξ for different values of Jeffrey Parameter λ_1 with $\lambda = 1, R = 1$.

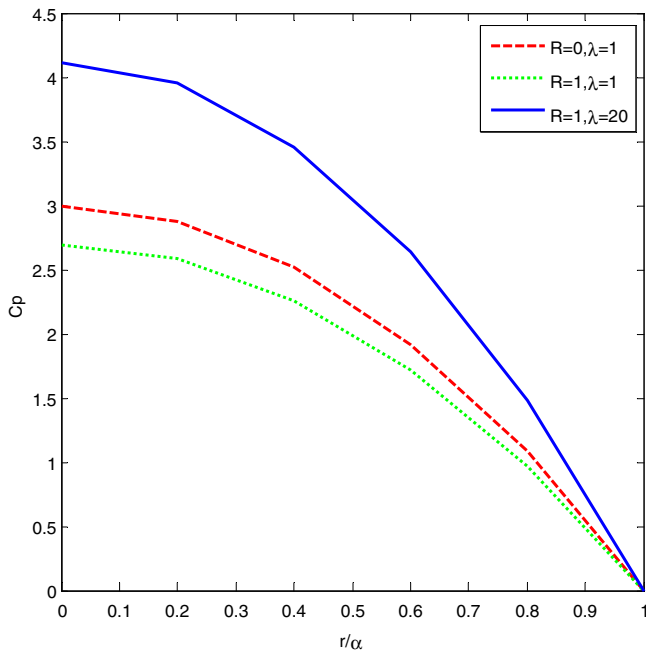


Figure 7. The variation of the pressure coefficient C_p with $\frac{r}{\alpha}$ for different values of Reynolds Number with $\lambda = 1, \lambda_1 = 0.1$.

Fig. 6 is sketched to find the effect of Jeffrey parameter on the radial velocity. We observe that radial velocity is decreasing with the increase of Jeffrey parameter λ_1 in the lower half of the region between the disks and the opposite phenomena is observed in the upper half of the region for fixed values $\lambda = 1$ and $R = 1$. Further the maximum radial velocity is shifting towards the upper disk (rotating) due to the increase in Jeffrey parameter λ_1 .

Fig. 7 is plotted to see the effect of the pressure coefficient C_p for fixed values $\lambda = 1$ and $\lambda_1 = 0.1$. It is noticed that the pressure coefficient increases with suction Reynolds number R decreases. The maximum pressure occurs at the stationary disk.

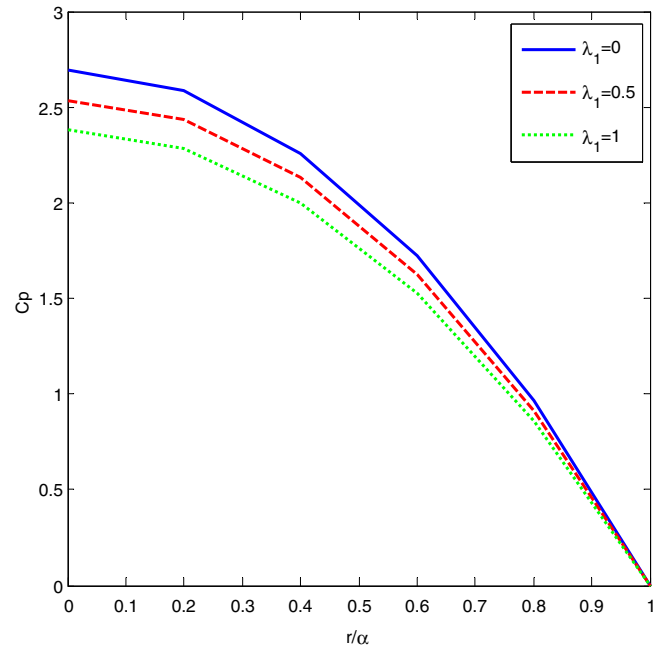


Figure 8. The Variation of the pressure coefficient C_p with $\frac{r}{\alpha}$ for different values of Jeffrey parameter λ_1 with $\lambda = 1, R = 1$.

Fig. 8 is sketched to see the effect of the pressure coefficient C_p for fixed values $\lambda = 1$ and $R = 1$. It is observed that the pressure coefficient decreases with the increase of Jeffrey parameter.

4. Conclusions

The three-dimensional flow of Jeffrey fluid bounded by two parallel disks, one rotating and another stationary with suction is discussed.

- Expressions for velocity, pressure and skin-friction have been obtained and compared with the creeping flow solutions.
- The radial velocity increases with the increases of Jeffrey parameter λ_1 .
- The axial velocity decreases with the increases of Jeffrey parameter λ_1 .
- The pressure coefficient decreases with the increase of Jeffrey parameter λ_1 .

References

- [1] Stewartson K. On the flow between two rotating coaxial disks. *Proc Comb Phil Soc* 1953;49:333–41.
- [2] Pearson CE. Numerical solutions of the time-dependent viscous flow between two rotating coaxial disks. *J Fluid Mech* 1965;21:623–33.
- [3] Elkouh AF. Laminar flow between porous disks. *J Eng Mech Div Proc ASCE* 1967; 93: EM4, 31.
- [4] Mellor GL, Chapple PJ, Stokes VK. On the flow between a rotating and a stationary disk. *J Fluid Mech* 1968;31:95–112.
- [5] Rudraiah N. Three dimensional flow between a rotating and a stationary disk with a uniform suction at the stationary disk. *PGSAM, (1969) PRSAM-1-6*.
- [6] Mishra SP, Acharya BP, Roy JS. Laminar elastico-viscous flow between rotating porous disks. *Revue Roumaine des Sciences Techniques, Series de Mecanique Appliquee* 1975;20(2):257–69.
- [7] Hayat T, Ahmad Niaz, Ali N. Effects of an endoscope and magnetic field on the peristalsis involving Jeffrey fluid. *Commun Nonlinear Sci Numer Simul* 2008;13(8):1581–91.
- [8] Sohail Nadeem, Sher Akbar Noreen, Naturforsch Z. Peristaltic flow of a Jeffrey fluid with variable viscosity in an asymmetric channel. *J Phys sci* 2009;64 (11):713–22.

- [9] Vajravelu K, Sreenadh S, Lakshminarayana P. The influence of heat transfer on peristaltic transport of a Jeffrey fluid in a vertical porous stratum. *Commun Nonlinear Sci Numer Simul* 2011;16(8):3107–25.
- [10] Farooq AA, Siddiqui AM, Rana MA, Haro T. A variant of the classical Von Kármán flow for a couple stress. *Fluid Chin Phys Lett* 2012;29:8.
- [11] Kavitha A, Reddy RH, Srinivas ANS, Sreenadh S, Saravana R. Peristaltic pumping of a Jeffrey fluid between porous walls with suction and injection. *Int J Mech Mater Eng (IJMME)* 2012;7(2):152–7.
- [12] Qayyum A, Awais M, Alsaedi A, Hayat T. Unsteady squeezing flow of Jeffrey fluid between two parallel disks. *Chin Phys Lett* 2012;29(3).
- [13] Ellahi R, Riaz A, Nadeem S, Musthtaq M. Series solutions of magnetohydrodynamic peristaltic flow of a Jeffrey fluid in eccentric cylinders. *Appl Math Inform Sci* 2013;7(4):1441–9.
- [14] Siddiqui AM, Farooq AA, Haroon T, Babcock BS. Variant of the classical von-Karman flow for a Jeffrey fluid. *Appl Math Sci* 2013;7(20):983–91.
- [15] Ellahi R, Rahman SU, Nadeem S. Blood flow of Jeffrey fluid in a catherized tapered artery with the suspension of nanoparticles. *Phys. Lett. A* 2014;378(40):2973–80.
- [16] Riaz A, Nadeem S, Ellahi R, Zeeshan A. Exact solution for peristaltic flow of Jeffrey fluid model in a three dimensional rectangular duct having slip at the walls. *J Appl Bionics Biomech* 2014;11:81–90.
- [17] Nadeem S, Riaz A, Ellahi R, Akbar NS. Mathematical model for the peristaltic flow of Jeffrey fluid with nanoparticles phenomenon through a rectangular duct. *Appl Nanosci* 2014;4:613–24.
- [18] Rashidi S, Dehgan M, Ellahi R, Riaz M. Study of stream wise transverse magnetic fluid flow with heat transfer around an obstacle embedded in a porous medium. *J Magn Magn Mater* 2015;378:128–37.
- [19] Nawaz M, Zeeshan A, Ellahi R. Joules and Newtonian heating effects on stagnation point flow over a stretching surface by means of genetic algorithm and Nelder – Mead method. *Int J Numer Method H* 2015;25:665–84.
- [20] Ellahi R, Shivanjan E, Abbasbandy S. Numerical study of magnetohydrodynamics generalized Couette flow of Eyring – Powell fluid with heat transfer and slip condition. *Int J Numer Method H* 2016;26(5):1433–45.
- [21] Bhatti MM, Ellahi R, Zeeshan A. Study of variable magnetic field on the peristaltic flow of Molecular Liquids. *J. Mol. Liq.* 2016;222:101–8.
- [22] Rahman SU, Ellahi R, Nadeem S, Zia QMZ. Simultaneous effects of nanoparticles and slip on Jeffrey fluid through tapered artery with mild stenosis. *J Mol Liq* 2016;218:484–93.